Article

Dimerization of linear butenes on zeolite supported Ni

Andreas Ehrmaier, Yue Liu, Stephan Peitz, Andreas Jentys, Ya-Huei (Cathy) Chin, Maricruz Sanchez-Sanchez, Ricardo Bermejo-Deval, and Johannes A. Lercher

ACS Catal., **Just Accepted Manuscript** • DOI: 10.1021/acscatal.8b03095 • Publication Date (Web): 29 Nov 2018

Dimerization of Linear Butenes on Zeolite Supported Ni^{2+}

Andreas Ehrmaier[1], Yue Liu[1], Stephan Peitz[2], Andreas Jentys[1], Ya-Huei (Cathy) Chin[1,3], Maricruz Sanchez-Sanchez[1] *, Ricardo Bermejo-Deval[1]*, Johannes Lercher*[1,4]

[1] Department of Chemistry and Catalysis Research Center, Technische Universität München, Lichtenbergstrasse 4, D-85747 Garching, Germany

[2] Evonik Performance Materials GmbH, 45772 Marl, Germany

[3] Department of Chemical Engineering and Applied Chemistry, University of Toronto, Toronto, Ontario M5S 3E5, Canada

[4] Institute for Integrated Catalysis, Pacific Northwest National Laboratory, P.O. Box 999, Richland, WA 99352, United States

ABSTRACT: Nickel and alkali earth modified LTA based zeolites catalyze the dimerization of 1-butene in the absence of Brønsted acid sites. The catalyst reaches over 95% selectivity to n-octenes and methylheptenes. The ratio of these two dimers is markedly influenced by the parallel isomerization of 1-butene to 2-butene, shifting the methylheptene/octene ratio from 0.7 to 1.4 as the conversion increased to 35 %. At this conversion, the thermodynamic equilibrium of 90 % cis- and trans 2-butenes was reached. Conversion of 2-butene results in methylheptene and dimethylhexene with rates that are one order of magnitude lower than with 1-butene. The catalyst is deactivated rapidly by strongly adsorbed products in the presence of 2-butene. The presence of π-allyl bound butene and Ni-alkyl intermediates were observed by IR spectroscopy, suggesting both to be reaction intermediates in isomerization and dimerization. Product distribution and apparent activation barriers suggest 1-butene dimerization to occur via a 1'-adsorption of the first butene molecule and a subsequent 1'- or 2'-insertion of the second butene to form octene and methylheptene, respectively. The reaction order of two for 1-butene and its high surface coverage suggest that the rate determining step involves two weakly adsorbed butene molecules in addition to the more strongly held butene.

KEYWORDS: *Linear alkenes; Nickel Lewis acid zeolite; dimerization; Nickel alkyl and LTA zeolite*

INTRODUCTION

Linear and single-branched alkenes and in particular octenes are important intermediates in the synthesis of high value products, such as co-monomers for low density polyethene.[1] The pathway to produce these molecules via dimerization is attractive, because it utilizes abundantly present light olefins. Nickel-based catalysts have been identified as the most promising family of catalytic materials, exhibiting a high activity and selectivity to linear alkenes.[2-7] These catalysts favor the formation of dimers and limit successive C-C bonding formation.

Mechanistically, α-alkene formation has been reported to occur via a Ni-alkyl complex, following the Cossee-Arlman mechanism, a metallacycles route, and proton-transfer mechanisms[8-10]. Catalysts based on Ni dispersed on solid supports, including molecular organic frameworks, were proposed to follow the former mechanism.[6, 11-18 19]

Indeed, ethene oligomerization over Ni exchanged zeolites has been proposed to proceed via formation of a 1' alkyl carbenium ion followed by a migratory insertion, while the products desorb with a ß-hydride elimination (Cossee-Arlman mechanism).[20] It has been suggested that the density of liquid-like ethene is required to aid the desorption of butene, limiting C_4 isomerization and further polymerization via ethene addition.[21]

To achieve high rates and to avoid side reactions, Ni^{2+} cations have to be well separated and the support should be free of other strong acid sites, in particular Brønsted acid sites (BAS). Mesoporous and microporous crystalline aluminosilicates and amorphous aluminosilicates are supports that can potentially achieve such high Ni dispersion,[22-29] provided that two Si-O-Al exchange sites are sufficiently close to stabilize a Ni^{2+} cation. Indeed, zeolites with high framework Al concentrations (Si/Al ~ 1-3) have been shown to be well suited. However, ion exchange with Ni^{2+} still leads frequently to isolated BAS that catalyze alkene dimerization to dimethylhexene, but also lead to isomerization, oligomerization and cracking.[30-33]

The importance to avoid isomerization is best illustrated with the fact that an additional pathway to branched alkenes is available for isomers with internal C=C bonds.[13, 15] In the case of dimerization of butenes, isomerization of 1-butene to 2-butene opens this pathway to undesired products.[34] Therefore, minimizing the relative rate of double bond isomerization is a critical challenge for dimerization of alkenes with more than three carbon atoms. Therefore, it is essential to combine a high concentration of isolated Ni^{2+} with the absence of Brønsted acid sites in order to achieve high selectivity to linear and single-branched alkenes. We have addressed this by choosing an LTA zeolite to host the Ni^{2+}, adjusting the other exchange cations not only to minimize or eliminate the presence of Brønsted acid sites, but also to adjust the electronic state of Ni^{2+}.

The present manuscript explores, therefore, partially Ni^{2+} exchanged Ca-LTA for butene dimerization. The narrow pores of LTA allow only the conversion at pore mouth or on the outer

surface. The rates of dimerization and competing isomerization are studied in the absence of Brønsted acid sites, combining characterization of adsorbed species by IR spectroscopy and kinetic measurements. This study shows a unique chemical environment for Ni^{+2}, weakening its Lewis acidity by coadsorption of a third butene molecule.

RESULTS AND DISCUSSION

1-Butene dimerization on Ni-Ca-LTA catalysts

At the start, a series of Ni-Ca-LTA-based catalysts with different Ni-loadings was prepared and characterized with respect morphology and crystallinity in order to select an adequate catalyst for mechanistic studies. Details are provided in the Supporting Information. Broadening of the XRD diffraction bands of LTA was observed with increasing Ni loadings (see SI, Figure S1), indicating certain loss of crystallinity due to the ion exchange.[35-36] While a hysteresis for the N_2 sorption was not observed for Ca-LTA (Figure S2), the sorption volume of the Ni containing catalysts showed important differences during adsorption and desorption, pointing to an increase of mesopore and a decrease of the micropore volume (Table S1). To minimize the impact of local lattice destruction, the loading of Ni was limited to 6 wt.% on Ni-Ca-LTA. Changes in the particle size were not observed by SEM (Figure S3 and Table S2).

Analysis by X-ray absorption spectroscopy (XAS) was used to establish the oxidation state of the Ni in Ni-Ca-LTA in contact with 1-butene. Variations in the Ni-K edge energy (8333 eV) prior and after exposure to 1-butene were not observed in the X-ray absorption near edge structure (XANES). This indicates that Ni is present as Ni^{2+} in the acting catalyst (Figure S4 A) and we conclude that Ni^{2+} is the active center for dimerization. [11, 37,38]

The weight based rate of 1-butene dimerization was determined for catalysts containing 2-6 % Ni (Figure S5, Table S3). The rate of dimerization increased linearly with the Ni concentration. This led us to conclude in turn that all (or a constant fraction) of Ni^{2+} is accessible to the reactants at this level of ion exchange. Therefore, the detailed mechanistic studies were performed on a 6 wt.% Ni exchanged Ni-Ca-LTA catalyst.

The butene conversion rates and product rate distribution upon time on stream for a 6 wt.% Ni exchanged Ca-LTA are shown in Figure 1. Rates in butene conversion were the highest within the first five hours ($1.5 \cdot 10^{-4}$ mol_C /g/s). These rates were less than an order of magnitude lower than rates reported for zeolites and mesoporous aluminosilicates with BAS.[11, 25-27] Subsequently, slight deactivation was observed with time on stream. For the mechanistic and kinetic studies in this work, the reported activity data were extrapolated to zero time on stream (TOS). Rates to octene and methylheptene were comparable ($6\text{-}7 \cdot 10^{-5}$ mol_C /g/s), while rates to dimethylhexene were of one order of magnitude lower. To compare the intrinsic dimerization and trimerization activity of Ni-Ca-LTA, we assumed an overall second order reaction for each pathway, i.e., second order in butene for dimerization and first order in both butene and octene for trimerization. A higher apparent second reaction order constant was observed for trimerization (k_{tri} = $5.67 \cdot 10^{-9}$ mol_C/g/s/bar^2) than for dimerization (k_{di} = $1.67 \cdot 10^{-9}$ mol_C/g/s/bar^2). Thus, Ni-Ca-LTA has a higher selectivity for trimers than for dimers in the oligomerization of 1-butene. This selectivity is higher than observed for Ni-aluminosilicates in the presence of Brønsted acid sites.[26] Note that the operating temperature below 200°C prevented cracking of 1-butene and products, as was observed with similar catalysts.[25]

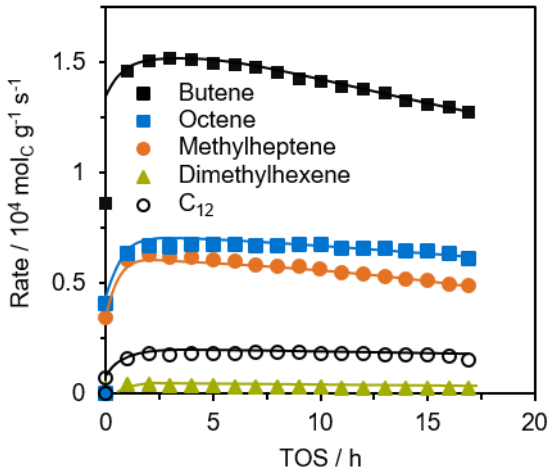

Figure 1. Reaction of 1-butene over a 6 wt.% Ni-Ca-LTA. Butene consumption rate (black squares) and formation rates of dimerization products over time on stream with respect to moles of carbon. T = 160 °C, p = 50 bar, WHSV = 38 h^{-1}.

Product distribution with Ni-Ca-LTA catalysts

The oligomerization of 1-butene on a 6 wt.% Ni containing LTA catalyst was conducted at 50 bar, 160 °C and space velocities ranging from 6 to 244 h^{-1} (Figure 2). Results show higher than 80 % selectivity towards octenes, with less than 20 % of higher oligomers – mostly trimers (not shown). Within the dimer fraction, the main products were 3-methylheptenes and n-octenes (Figure 1 and Figure 2 A). Only small amounts (less than 5 % among the dimers) of 3,4-dimethylhexenes were formed. The thermodynamic dimer equilibrium at the given conditions predicts a ratio of dimethylhexene / methylheptene / octene of 34 / 60 / 6 (Figure S6 in SI), i.e., the products observed are quite distant from equilibrium.

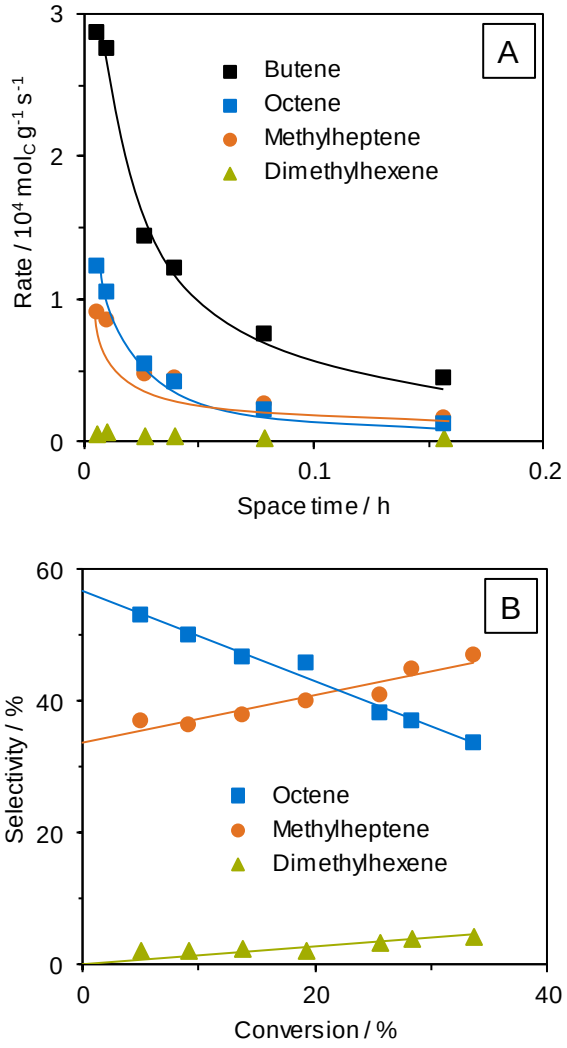

Figure 2. A) Effect of space time on catalytic conversion rate of 1-butene (black squares) and dimer distribution, and B) Dimer selectivity as a function of the conversion of 1-butene over a 6 wt.% Ni-Ca-LTA catalyst. T = 160 °C, p = 50 bar, WHSV = 6-245 h^{-1}.

The 1-butene consumption rate with varying space time is shown in Figure 2 A. Upon higher space times, 1-butene consumption leveled off at a rate of $5 \cdot 10^{-5}$ mol_C /g/s, corresponding to ca. 35 % conversion. It was not possible to surpass this level of conversion by an increase in space time. However, this value is far from the dimerization thermodynamic equilibrium (close to 100 % 1-butene conversion as shown in Figure S6 in SI). As the conversion increased, 1-butene was isomerized to 2-butene, reaching the thermodynamic equilibrium (Figure 3 A) at the point (Figure 2 A) when the 1-butene conversion rate in dimerization leveled off, at approx. $5 \cdot 10^{-5}$ mol_C /g/s (conversion values of ~30-35 %, grey bar in Figure 3 A). Figure 3B shows the approach to equilibrium for the two parallel reactions: dimerization and butene double bond isomerization (defined as the ratio of the different isomers, see SI for details). Isomerization increased rapidly to the value of one with butene conversion, indicating equilibration, while dimerization did not exceed the value of 0.35 (Figure 3B). Therefore, it is suggested that double bond isomerization, i.e., the increasing concentration of 2-butene, limits the conversion level.

The dimer selectivity as a function of 1-butene conversion is shown in Figure 2 B. Methylheptene and octene were the predominant products of 1-butene dimerization, while dimethylhexene was formed in significantly lower concentrations. The changes in dimer product selectivity and the double bond isomerization with butene conversion show that octene is formed solely from 1-butene, and that dimethylhexene is solely formed from 2-butene dimerization.

Methylheptene can be formed from both 1- and 2-butene. Scheme 1 shows the reaction pathways proposed for the dimerization of 1-butene. The adsorption of the first butene molecule on the Ni active site is hypothesized to take place at the primary (1'-adsorption) or at the secondary carbon atom (2'-adsorption).[20, 39-42] The insertion of the second butene for C-C bond formation, can also take place at the primary (1'-insertion) or secondary (2'-insertion) carbon. The modes of adsorption and insertion and their probability determine the selectivity to the dimer isomers (octene, 3-methylheptene and 3,4-dimethylhexene). The obtained product distribution indicates that the main route in dimerization with Ni-Ca-LTA takes place either by 1'-adsorption of 1-butene and 1'-insertion or 2'-insertion of 1-butene, because n-octene and methylheptene were formed preferentially.

At higher conversions, the increase in selectivity to methylheptene and dimethylhexene is attributed to a higher contribution of the 2'-adsorption and/or 2'-insertion pathway. This is speculated to be also the result of a higher 2-butene concentration from the double bond isomerization of 1-butene (the options for 2-butene are shown in green color in Scheme 1). Therefore, octene and methylheptene are concluded to be primary products, dimethylhexene to be a secondary product. It is noted in passing that, the absence of Brønsted acid sites (BAS) is responsible for the low dimethylhexene selectivity. In presence of the latter formation of dimethylhexene (selectivity above 30%) is favored by the formation of secondary carbenium ions. [11, 28, 37, 43]

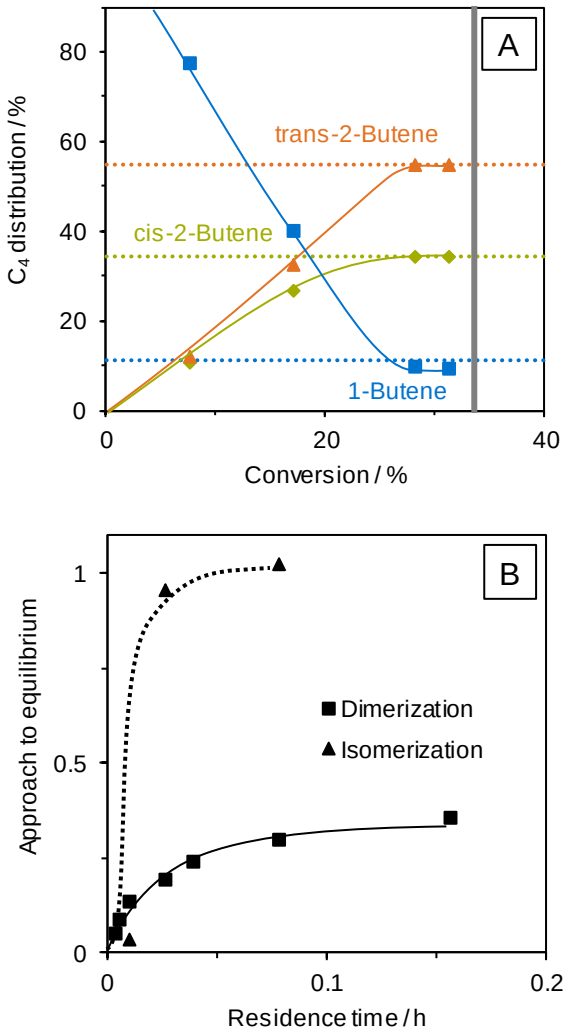

Figure 3. A) Reactant isomerization behavior over 6 wt.% Ni-Ca-LTA. The dotted lines give the equilibrium at 50 bar and 160 °C. B) Approach-to-equilibrium for dimerization and isomerization. Reaction conditions: T = 160 °C, p = 50 bar, WHSV = 6-245 h^{-1}.

Impact of 2-butene on the deactivation of Ni-Ca-LTA

The limiting butene conversion of 35 % (leveling off at a rate of $5 \cdot 10^{-5}$ mol_C /g/s, Figure 1) and chemically equilibrated double bond isomerization, taken together, suggest that 2-butene hinders further dimer formation (Figure 3). To test this hypothesis, pure cis-2-butene was fed and oligomerized (Figure 4). With cis-2-butene, rates were significantly lower and decreased much more rapidly (Figure 4A), as well as higher selectivities to methylheptene and slightly higher selectivities to dimethylhexene (Figure 4B) were observed. Therefore, following the reaction pathway of Scheme 1, 2-butene can only adsorb via 2'-adsorption (Scheme 1, green color), leading to branched products only. The fact that n-octene was also formed even at lower conversions, suggests that a small fraction of 2-butene was isomerized to 1-butene, which in turn acted as precursor to n-octene.

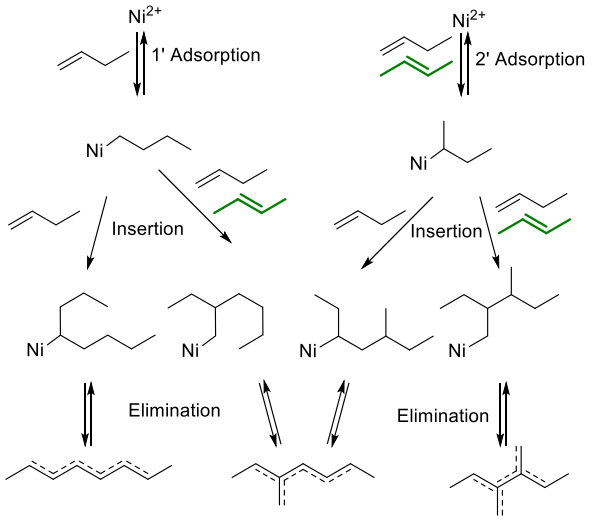

Scheme 1. Possible pathway for the formation of the dimer isomers from 1-butene (black) and 2-butene (green). Adapted from Cossee-Arlman mechanism.[39]

In order to understand the low activity of Ni-Ca-LTA in the dimerization of 2-butenes, the feed was switched between 1- and 2-butene (Figure 5). The first transient from 1-butene to cis-2-butene (Figure 5A) led to a rapid decrease in butene conversion rate. In a second experiment, the reactor was first fed with 2-butene and subsequently switched to 1-butene. This transient increased the dimerization activity, but to a level that was approximately one order of magnitude lower than that starting from 1-butene (Figure 5B, and comparison to 5A). Thus, we conclude that 2-butene induced irreversible changes to the most active sites of Ni-Ca-LTA.

Based on the above results, we conclude that 1-butene isomerizes to 2-butene, inducing rapid deactivation, especially at higher conversions. The higher concentration of 2-butene compared to 1-butene (90 % 2-butene and 10 % 1-butene at conversions above 30 %, Figure 3 A) leads also an increase in the selectivity to products formed from the 2'-adsorption pathway, i.e., methylheptene and dimethylhexene (Figure 2 B). However, the selectivity to n-octene is still higher than that to dimethylhexene, indicating a significantly faster dimerization for 1-butene than for 2-butene.

The low activity in 2-butene dimerization is hypothesized to be caused by the formation of a stable Ni-alkyl species either via the 2'-adsorption or via the insertion of another alkene (1-butene or 2-butene) into the secondary carbon of the adsorbed 2-butene. Thus, the deactivation over time observed in Figure 1 is concluded to be caused by the high concentration of 2-butene (ca. 2/3 of butene at 20% butene conversion), leading to the formation of a surface species that is unable to desorb.

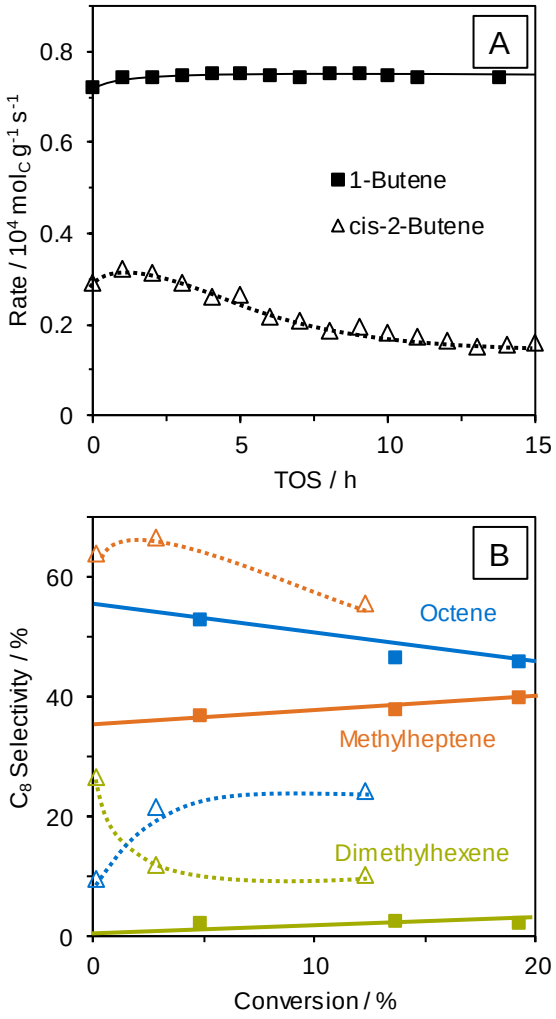

Figure 4. Conversion rate, in terms of the moles of carbon (A), and product distributions (B) of 1-butene and cis-2-butene dimerization reaction over 6 wt.% Ni-Ca-LTA at 160 °C, 50 bar, WHSV graph A = 12.5 h^{-1}; WHSV graph B =12-245 h^{-1}. Conversion of cis-2-butene is shown as empty triangles, reaction of 1-butene is presented as filled squares, and so are the corresponding products. Colors of products: n-octene (blue), methylheptene (orange), dimethylhexene (green).

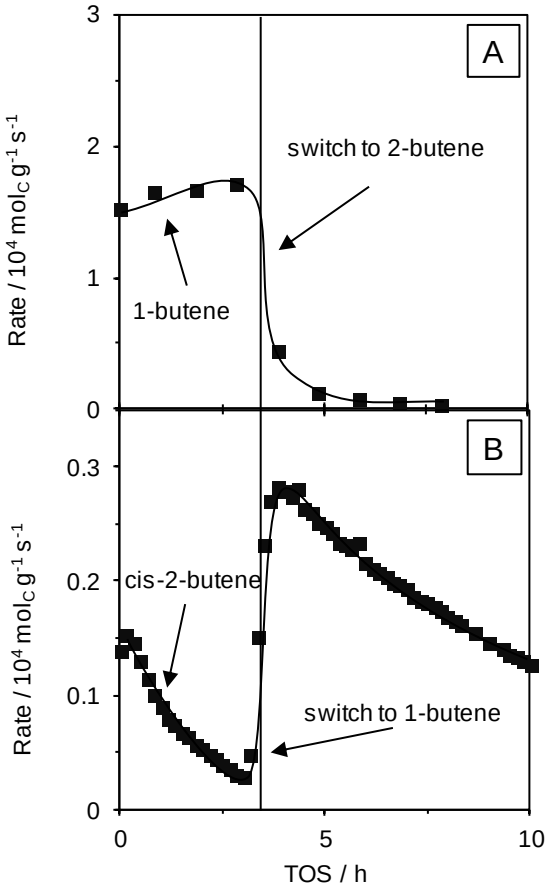

Figure 5. Effect of cis-2-butene on butene consumption rate over a 6 wt.% Ni-Ca-LTA, at T = 160 °C and P = 50 bar, starting with 1-butene and switched to cis-2-butene (WHSV = 50 h^{-1}) (A), and experiment started with cis-2-butene and switched to 1-butene (WHSV = 50 h^{-1}) (B).

To analyze the carbonaceous deposits resulting from exposure to 2-butenes, spent catalysts were dissolved in HF and the remainder was subsequently dried at 90 °C. The organic residue was dissolved in hexane and analyzed by gas chromatography. A higher concentration of C_{16+} was observed after 2-butene dimerization, while concentrations of hydrocarbons between C_{12} and C_{16+} were similar to those obtained after 1-butene dimerization. This suggests that 2-butene dimerization forms larger oligomers that block and deactivate Ni^{2+} sites.

Kinetics of 1-butene dimerization

The reaction orders obtained for the formation of octene and methylheptene (Figure 6), with respect to 1-butene, were approximately 2 (Figure S7 C and D). This points to the C-C coupling of the two weakly adsorbed butenes as the rate determining step (r.d.s.), in agreement to studies on ethene dimerization.[21, 44-46] The measured activation energies for the formation of the specific dimers, as well as for the different oligomers, are shown in Table 1 (Arrhenius plots are shown in Figure S7 A and B in SI). The reaction order and activation energy were not measured for dimethylhexene, since it is a secondary product. Among the dimers, the values of apparent activation energies

(E_a) determined for methylheptene and octene were similar (76 and 72 kJ/mol, respectively) and indicate that both products stem from a pathway with a similar transition state. The values were similar to the ones obtained by Zhang et al. with Ni-ZSM-5.[47] As previously shown in Scheme 1, the formation of dimethylhexene requires the 2'adsorption and 2'insertion of 1-butene or 2-butene. Therefore, prior to the formation of dimethylhexene, isomerization of 1-butene into 2-butene must take place.

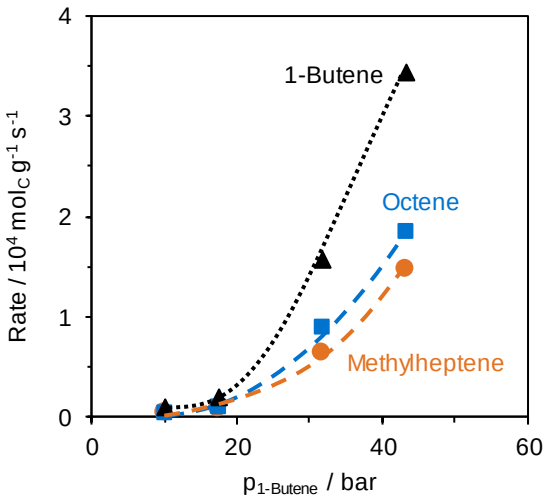

Figure 6. Reaction of 1-butene consumption and formation of methylheptene and octene over 6 wt.% Ni-Ca-LTA.. T = 160 °C, p = 50 bar, WHSV = 15-156 h^{-1}; 1-Butene feed mix diluted with propane: $c_{1\text{-butene}}$ = 20 – 86 wt.%.

Table 1. Energy of activation for the butene consumption, as well as for the formation of products at conversion levels between 0.5 and 3.5 %. WHSV = 150 h^{-1}, p = 50 bar, T = 140-180 °C. Arrhenius plots are shown in SI (Figure S7).

	E_A [kJ mol^{-1}]
C_4 consumption	73
Methylheptene	76
Octene	72

IR spectra of adsorbed and reacted butenes

IR spectroscopy is used to characterize the adsorbed species and monitor the gradual isomerization of adsorbed butenes as reaction proceeds. The basic nature of the catalysts stabilizes carbonates, which change in nature and concentration during reaction. We hypothesize that these carbonates are largely spectators to the catalytic transformations. However, their presence will moderate the acid-base properties of the investigated catalysts.

Exposing the activated zeolites to 1-butene and subsequent evacuation led to IR spectra of adsorbed 1-butene on Ca-LTA and Ni-Ca-LTA that are compiled together with the assignments in SI-5 (Table S4, Figure S8, and Figure S9). The spectra of 1-butene adsorbed on Ca-LTA and Ni-Ca-LTA showed bands at 1300-1700 cm^{-1} (Figure S8), which are characteristic of C=C stretching, C-H bending and carbonate or carboxylate vibrations. The assignments and the discussion on the carbonate bands are provided in SI-5. The IR spectra of 1-butene adsorption on Ca-LTA and Ni-Ca-LTA in the 2700-3200 cm^{-1} region are shown in Figure S9. Admission of butene leads to C-H stretching bands on both samples. The bands at above 3000 cm^{-1} are attributed to C-H stretching vibrations at C=C bonds, while the bands below 3000 cm^{-1} are attributed to C-H vibrations at C-C bonds of physisorbed alkenes.[48-49]

After activation of Ni-Ca-LTA, 1-butene was adsorbed at constant pressure (1 mbar) and IR spectra (Figure 7) showed bands characteristic of bidentate carbonate as described in SI-5. The most pronounced bands between 1620 and 1660 cm^{-1} are assigned to π-bonded butene on Ni^{2+}. Directly after exposing the sample to a stream of 1-butene, a band at 1622 cm^{-1} with a shoulder at 1658 cm^{-1} (attributed to gaseous 1-butene[50]) was observed. The wavenumber at 1622 cm^{-1} tentatively attributed to π-bonded 1-butene.[48, 51-52] After 10 min, a band at 1641 cm^{-1} evolved. It is attributed to an adsorbed alkene with an internal double bond (π-bound 2-butene or a branched octene), since the higher wavenumber indicates a stronger C=C bond for 2-butene than for the external C=C bond observed for 1-butene (1622 cm^{-1}).[50, 53] This is further supported by the variations of the relative intensity of the CH vibrations at 1440, 1408, 3061 and 3005 cm^{-1} (Figure 7), indicating an increasing number of =CH vibrations in the surface species.

The changes observed in the concentration of methyl groups of the adsorbed hydrocarbons allowed us to follow double bond isomerization and/or dimerization reactions of 1-butene. An increase in the intensity of CH_3 group vibration (1390 cm^{-1}, Figure 7A), especially within the first 30 min, and in the CH_3 bending vibration (2873 and 2967 cm^{-1}, Figure 7B), suggests that several CH_3 groups were formed, as the combined result of isomerization and alkene addition. Because the intensity of the CH_2 bands (2841 and 2939 cm^{-1}) remained constant throughout the experiment, we conclude that double bond isomerization and the formation of surface alkyl species are the main surface reactions under these conditions. Within the 30 min of exposure, two additional bands appeared at 1585 and 1295 cm^{-1}. The lower wavenumber is attributed to a delocalized C=C bond stretching vibration, tentatively assigned to π-allyl formation.[54] In addition, the band at 1295 cm^{-1} is assigned to the stretching of a carbenium ion (ν_{as} C^+-C).[55-57] The allyl species is hypothesized to lead to isomerization, while the carbenium ion is suggested to be a key intermediate in the dimerization (Scheme 2).

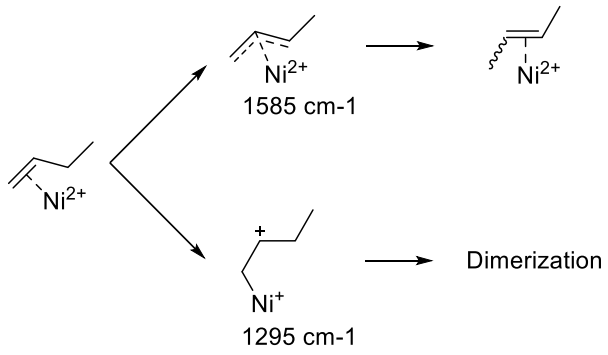

Scheme 2. Surface intermediates detected upon butene adsorption on Ni-Ca-LTA and their proposed reactivity.

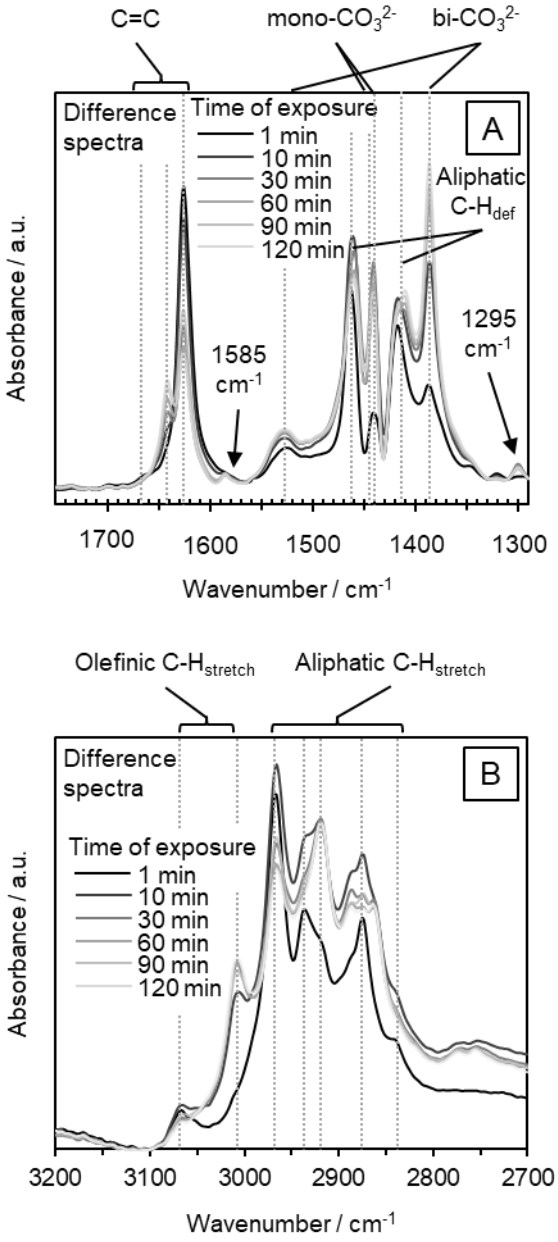

Figure 7. IR spectra of 6 wt.% Ni-Ca-LTA at 40 °C exposed to 1 mbar of 1-butene after 1-30 minutes A) 1300-1700 cm^{-1} range, B) 2700-3200 cm^{-1} range.

Enthalpic contribution of adsorption of butenes on Ni-Ca-LTA

The heat of adsorption of 1-butene on Ni-Ca-LTA was of 63 kJ mol^{-1} (Figure S10). A Langmuir approach was used to fit the isotherm, with a maximum surface coverage of 0.73 $mmol_{1\text{-butene}}/g$ and an adsorption constant K of $4.9 \cdot 10^{-3}$ bar^{-1} (SI-6) at 40 °C. This adsorption constant at 40 °C gives the adsorption constant of $6.0 \cdot 10^{-6}$ bar^{-1} at 160 °C, according to van't Hoff equation (SI-6). This adsorption constant translates to Ni^{2+} sites nearly saturated with 1-butene, as predicted by Langmuir adsorption isotherm ($P_{1\text{-butene}}$ = 42.5 bar). The high adsorption enthalpy of 63 kJ mol^{-1} indicates a strong interaction of the alkene

with the Ni, leading to the formation of a Ni alkene complex, potentially increasing the electron density at Ni^{2+}. It should be noted in passing that this hypothesized interaction was not manifested in XANES at the Ni-K edge energy (8333 eV).

The adsorption of 2-butene was also examined (Figure S11). A successive weight increase was observed within the first 12 hours at 0.03 mbar of 2-butene. The initial adsorption enthalpy was, however, approximately 63 $kJmol^{-1}$ and hence similar than for 1-butene.

Catalytic pathway of butene dimerization on Ni-Ca-LTA

The product distribution and the concluded formation of a Ni-alkyl complex (Scheme 1) are compatible with the proposed dimerization mechanism. The obtained product distribution indicates the dimerization is mainly taking place by 1'-adsorption of 1-butene and 1'-insertion or 2'-insertion of 1-butene, because n-octene and methylheptene were formed preferentially. In contrast, a metallacycle mechanism would involve the formation of the three dimers in comparable concentrations. Their ratio would depend on the adsorption and insertion orientation of the π-bound alkenes.[58-59] The very low formation rates of dimethylhexene and its non-existence at 0 % conversion led us to conclude that the metallacycle mechanism is not operative for Ni-Ca-LTA.

The product distribution obtained on Ni-Ca-LTA points to a stepwise mechanism for butene dimerization. We propose a dimerization pathway adapted from Cossee-Arlman mechanism (Scheme 3), which involves initially the formation of a Ni-alkyl complex as the active site throughout the entire catalytic cycle (Scheme 3). The full coverage of Ni by 1-butene and the reaction order of 2 with respect to 1-butene support the formation of a Ni-alkyl complex as the active site; this site is able to coordinate to two additional butene molecules that lead to the dimer. The catalytic cycle begins with the adsorption of 1-butene on the Ni-alkyl complex, preceded by the formation of a covalent bond with the Ni-alkyl complex (Step 1, Scheme 3), in chemical equilibrium with the gas phase butene. We view the allyl complex as the intermediate for the isomerization of π-bonded 1- and 2-butene on Ni (Scheme 2). In the next step, a second butene molecule weakly adsorbs via π bond interaction. Consecutively, the third step is the kinetically relevant C-C bond formation that forms the C_8 alkene product (step 3 in Scheme 3). Desorption of the C_8 alkene regenerates the Ni-$alkyl_{C4}$ complex, making it ready for the next catalytic cycle. Pseudo steady-state treatments on the intermediates, together with assumptions of binding site and Ni-alkyl complex as the most abundant surface intermediates (step 1, Scheme 3), give the rate expression of (derivation at SI-4):

$$r = \frac{K_1 K_2 k_3 [C_4]^2}{1 + K_1[C_4] + K_2[C_4] + [C_8]/K_4} \approx k[C_4]^2$$

which simplifies to an apparent 2nd order dependence at low surface coverages in the limit of low product concentration. The K and k are the equilibrium constants for adsorption and elementary C-C bond formation rate constant of the kinetically relevant step, as also defined in Scheme 3.

It should be noted that, according to Scheme 3, an internal hydride shift (step 3a) is necessary, before the products can desorb from the Ni site and regenerate the active site to form a new Ni-alkyl complex. Brogaard et al.[20] have estimated that Ni-alkene-alkyl complexes of different alkyl chain length are quite close in free energy in the Cossee-Arlman pathway. Similarly, the proposed mechanism suggests the change to a larger adsorbate for the Ni-alkene-alkyl complex, evolving from a Ni-alkene-$alkyl_{C4}$ to a Ni—alkene-$alkyl_{C8}$. The reason for this modified Cossee-Arlman mechanism on Ni-zeolite is attributed to the absence of Brønsted acid sites.[20] The lack of Brønsted acidity also agrees well within the high yields to linear and mono-branched C8 isomers, because dibranched dimer are favored by Brønsted acid catalyzed dimerization.[32-33]

While this is a plausible mechanistic pathway, the strong adsorption of butene on Ni^{2+} and the chemical potential of the reacting butene suggest that the reaction starts from a Ni-alkyl complex. This complex is equivalent to those observed in homogeneous systems,[8] having ligands coordinated to Ni metal altering the electronic charge of its d orbital. The observed second-order and the full coverage requires to postulate the presence of this Ni alkene complex that moderates the coordination of the reacting butenes with Ni^{2+}.

The insertion step defines the product selectivity upon the orientation of the adsorbed butene molecule. The possible orientations of the butene molecules within the cyclic transition state are shown in Scheme S1 in SI, as those proposed by theory with Ni homogeneous complexes.[44] In this case it is proposed a relatively low stability of the primary carbenium ion that would be formed upon a 2'-adsorption of 1-butene (Scheme S1 B in SI). Hence, it is preferred an initial 1'-adsorption of pure 1-butene. Once 2-butene is available from the double bond isomerization of 1-butene, 2'-adsorption of 2-butene leads to a better stabilized secondary carbenium ion, which opens another dimerization pathway via this intermediate. In all cases, however, the butene insertion step is associated with the highest activation barrier.

CONCLUSION

1-Butene dimerization on a Ni-Ca-LTA derived catalysts was highly selective to methylheptene and n-octene (95%), shifting the methylheptene/octene ratio from 0.7 to 1.4, in the conversion range up to 35 %. The main dimerization pathway is proposed to take place via initial 1'-adsorption of 1-butene on Ni and subsequent 1- or 2-insertion of a second butene, leading to the high selectivity to methylheptene and n-octene dimers.

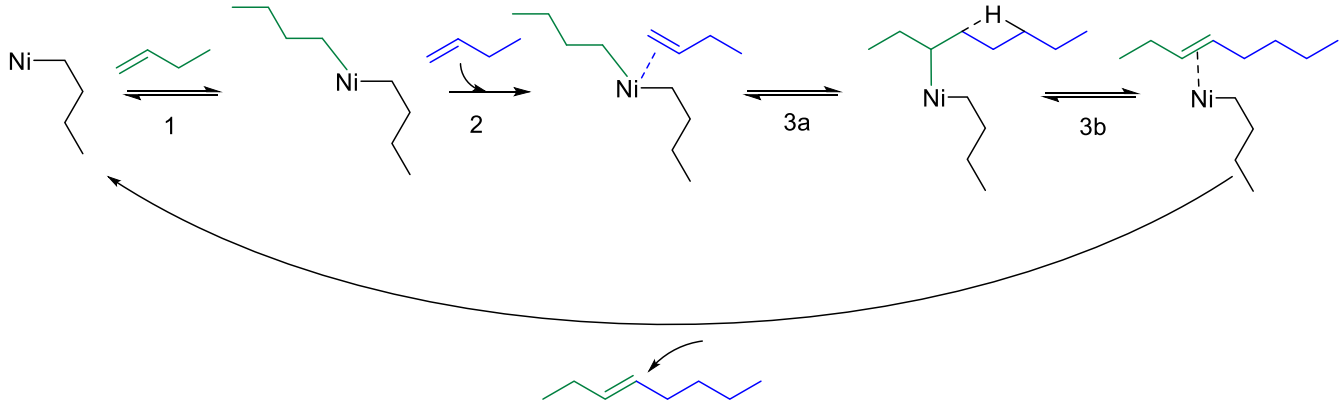

Scheme 3. Proposed reaction network for dimerization of linear butenes over Ni active site (Ni-alkyl in the zeolite). Firstly, 1-butene (green) would adsorb on the Ni-alkyl complex (1). A second butene molecule (blue) weakly adsorbs on the Ni-alkyl$_{C4}$ complex (2). Collectively, dimerization is taking place on the Ni-alkyl$_{C8}$ complex (3), being rate limiting. Finally, there is a subsequent internal hydride shift, leading to product desorption from the Ni site and formation of the Ni-alkyl$_{C4}$ complex for a new catalytic cycle.

Double bond isomerization of butene is also catalyzed by Ni^{2+} in Ni-Ca-LTA. The extent of dimerization plays an important role for the dimerization pathway. High concentrations of 2-butene favor the 2'-insertion into 1'-adsorbed species, increasing the selectivity to methylheptene. The 2'-adsorption is the only possible mode for internal alkenes, causing a high concentration of 2'-adsorbed species and lead to the formation of mono- and dibranched dimers. Double bond isomerization equilibrium was reached at about 30% conversion and limited the conversion rate to dimers by almost one order of magnitude. Adsorbed 2-butene or its dimerization products also lead to irreversible changes at the active sites and blocking them by formation of strongly bound oligomers.

IR spectroscopy shows that Ni-allyl and Ni-alkyl complexes are formed as most abundant intermediates during isomerization and dimerization. During isomerization, the adsorption-desorption is equilibrated and the reactants assume an allylic transition state.

Dimerization of linear butenes on Ni-Ca-LTA follows a Cossee-Arlman type mechanism. After formation of the Ni-alkyl complex, two butene molecules form a C-C bond. Ni sites are interacting with 1-butene, forming Ni-alkyl complexes, at which a second order kinetically-relevant C-C bond formation occurs that leads to octenes. These findings suggest the Ni^{2+} species that catalyzes the reaction exists in a very special chemical environment involving an additional coordinated butene.

EXPERIMENTAL

Catalyst preparation. Ca-LTA was obtained by stirring Ca-LTA-5A (Sigma-Aldrich, pre-calcined: 4 h, rate 5 °C/min, 500 °C) with water (20 g_{water} / $g_{zeolite}$) at 80 °C for 24 h (pH = 7-8 over total exchange time). The solid was recovered and washed thoroughly with deionized water. After drying at 100 °C for 10 hours, the precursor was calcined (8 h, rate: 5 °C/min, 500 °C, air). Ni-Ca-LTA with different Ni wt.% was prepared by aqueous ion exchange of Ca-LTA-5A with Ni^{2+}. The Ni^{2+} ion exchange was carried out with an aqueous $Ni(NO_3)_2$ (Sigma-Aldrich) solution (20 $g_{solution}$ / $g_{zeolite}$) at 80 °C for 24 h. The molarity of the solution varied between 0.00-0.06 M to obtain 0-6 wt.% Ni^{2+} in Ca-LTA (0 wt.% of Ni^{2+} was obtained in the case of no $Ni(NO_3)_2$ in solution). During Ni ion exchange, the pH value was 6-7 during the total time of exchange (Figure S12). The charge balance was approximately 100% with respect to Al atoms (Table S5). The solid was recovered and washed thoroughly with deionized water. After drying at 100 °C overnight, the precursor was calcined (8 h, rate: 5 °C/min, 500 °C, air).

Characterization methods. Two different methods were followed in the adsorption of 1-butene on Ni-Ca-LTA via IR: 1-butene was adsorbed, equilibrated and subsequently evacuated stepwise; and the time resolved adsorption of 1-butene at a constant pressure. In the first method, low pressure IR spectra were recorded on a Vertex 70 spectrometer from Bruker Optics, equipped with a liquid nitrogen cooled detector. A thin and self-supporting wafer was installed and activated for 1 h at 450 °C (rate: 10 °C/min) in vacuum. After cooling to 40 °C, butene was adsorbed to 0.5 mbar and then later evacuated ($P < 10^{-7}$ mbar). Scans were taken with a resolution of 0.4 cm^{-1}, with an average of 120 scans per spectrum. In the second approach, for IR spectroscopy under constant pressure, the samples were prepared as self-supporting wafer and first activated in vacuum at 450 °C (rate: 10 °C/min) in situ for 2 h. After pretreatment, the activated samples were cooled to 40°C. Subsequently, 1-butene was adsorbed at 1mbar. Spectra were recorded after 1-30 minutes on a Nicolet iS50AEM spectrometer from ThermoScientific, equipped with a liquid nitrogen cooled detector at a resolution of 4 cm^{-1}. Scans were taken from 1000-4500 cm^{-1} with an average of 500 scans per spectrum.

For determining the coke, spent catalysts (24 h on stream at 160 °C and 50 bar, WHSV = 50 h^{-1}) were dissolved in a sufficient amount (approx.. 20 ml) of HF at 80 °C. After evaporation of

HF, the residue was collected in hexane and injected into a GC equipped with a 50 m HP-1 column and a flame ionization detector.

X-ray diffraction (XRD) measurements were performed in a PANalytical Empyreal System diffractometer, equipped with a Cu- Kα radiation source ($K\alpha_1$ line of 1.54 Å; 45 kV and 40 mA)). The diffractograms were measured by the usage of a sample spinner stage in a 2θ range between 5 ° and 70 ° (step size: 0.0131303/2θ) at ambient conditions.

X-ray absorption (XAS) spectra were recorded at DESY in Hamburg, Germany at PETRA III, P65. The monochromatic photon flux was at $2x10^{12}$ s^{-1} at 9 keV and a beam size of 0.5x1 mm^2. The sample was packed in a in-situ XAS setup capillary and activated in 10 % O_2 in He flow (5 ml/min) at 450 °C (rate: 10 °C/min) for 2 h. After cooling down to 160 °C, the system was flushed with He, before 1-butene flow (1.5 ml/min) was loaded for 4 h at 160 °C and ambient pressure. The spectra were recorded between 8160 and 8700 eV and evaluated in Athena software.[60] For the linear combination fit, NiO and Ni foil were applied as standards for Ni^{2+} and Ni^0, respectively.

For the determination of the particle size, the catalyst particles were enhanced (magnification: x2000) by a high resolution JEOL JSM-7500F scanning electron microscope (voltage: 2 kV) and subsequently measured. For the sample preparation a small amount of catalyst was sonicated in EtOH, dropped on the sample Cu grid and dried at ambient conditions.

The gravimetric sorption isotherms of 1-butene and 2-butene on Ni-Ca-LTA was measured in a Setaram TG-DSC 111 thermoanalyzer connected to a high vacuum system. About 20 mg of sample was placed in a quartz crucible and activated at 450 °C (rate: 10 °C/min) for 1 h in vacuum ($p < 10^{-4}$ mbar). After cooling to 40 °C, the sample was exposed to 1-butene in small pressure steps from 0.01 to 10 mbar. Both, the sample mass and the thermal flux were monitored. The heat of adsorption was directly obtained by integration of the observed heat flux signal. During the adsorption of 2-butene on Ni-Ca-LTA a successive weight increase was observed during the first 12 hours at 03 mbar of 2-butene. The adsorption enthalpy was directly obtained by integration of the heat flux signal for the same time interval as 1-butene.

The BET specific surface area and pore volume of the zeolite were determined by nitrogen physisorption. The isotherms were measured at liquid nitrogen temperature (77 K) using a PMI Automatic Sorptometer. The catalyst was activated in vacuum at 473 K for 2 h before measurement. Apparent surface area was calculated by applying the Brunauer-Emmett-Teller (BET) theory with a linear regression between p/p_0 = 0.01 – 0.15. The micro- and mesopores were determined from the t-plot linear regression for t = 5-6 Å.

Catalytic testing and reaction kinetics. Catalytic tests were conducted in a fixed bed plug flow reactor (PFR (id = 3.9 mm)), connected to an online GC analysis unit (Agilent HP 6890, equipped with a 50 m HP-1 column). Prior to GC analysis, hydrogen is added to the product stream, which is hydrogenated over a Pt/Al_2O_3 catalyst. A mixture of 15 % i-butane and 85 % 1-butene is introduced by a syringe pump (ISCO model 500 D), temperature is controlled by a eurotherm 2416, pressure is controlled using a Tescom backpressure regulator.

Prior to weighing, the catalyst was dried at 100 °C for 1 h. The catalyst bed is diluted with SiC and fixed in the isothermal zone of the reactor. After activation for 2 h at 450 °C (rate: 10 °C/min) in air, the system is purged with nitrogen and pressurized to the desired pressure. Subsequently the system is flushed with the feed mixture (5 ml/min) for 2 min. After the desired flow rate is set, temperature program and GC measurements are started.

Standard measurement conditions were at 160 °C and 50 bar with a flow rate of butene mixture between 0.04 and 0.12 ml/min. These reaction conditions resulted in higher activity and lower deactivation. Catalyst loading was varied between 10 and 200 mg. WHSV was in the range 6 to 244 g g^{-1} h^{-1}.

Activation energy was determined between 140 and 180 °C at 50 bar with a WHSV of 150 h^{-1}. Reaction order was measured at 50 bar total pressure, 160 °C and WHSV of butene of 25 h^{-1}. The feed was diluted with propane, which led to concentrations of 1-butene between 32 and 86 wt.%.

i-Butane is inert under reaction conditions applied, and hence it was used as internal standard for normalization of GC areas. Conversion, selectivity and yield are calculated according to following equations:

$$X = \frac{n(butene)_{in} - n(butene)_{out}}{n(butene)_{in}}$$

$$S = \frac{n(product)_{out}}{n(butene)_{in} - n(butene)_{out}} \frac{|\nu_{butene}|}{\nu_{product}}$$

$$Y = \frac{n(product)_{out}}{n(butene)_{in}} \frac{|\nu_{butene}|}{\nu_{product}}$$

ASSOCIATED CONTENT

Supporting Information. Supporting information is available free of charge via the Internet at http://pubs.acs.org."

Additional graphs, experimental details, characterization data, thermodynamic equilibrium data, considerations on approach to equilibrium and reaction kinetics, additional reaction schemes.

AUTHOR INFORMATION

Corresponding Author

*m.sanchez@tum.de
*ricardo.bermejo@tum.de
*johannes.lercher@tum.de

ACKNOWLEDGMENT

This work was funded by EVONIK Performance Materials GmbH. J.A.L. acknowledges support for their contribution by the U.S. Department of Energy (DOE) (CN 269409), Office of Science, Office of Basic Energy Sciences, Division of Chemical Sciences, Geosciences & Biosciences for exploring transition metal cations for C-C bond forming reactions. R.B.D acknowledges the Alexander von Humboldt foundation for financial support.

ABBREVIATIONS

Al, aluminum; Å, Angström; BAS, Brønsted acid sites; BET, Brunauer-Emmett-Teller; C_4, butenes; C_8, octenes; C_{12}, dodecenes; C_{16}, hexadecenes; Ca, calcium; Ca-LTA, Ca-containing LTA, Ca-LTA-5A, commercial zeolite 5 A, LTA, Linde Type A zeolite; Cu, copper; E_a, energy of activation; EtOH, ethanol; eV, electron volts; GC, gas chromatograph; g, gram catalyst; h, hour; HF, hydrogen fluoride; IR, infrared; k_{di}, rate constant for dimerization; k_{tri}, rate constant for trimerization; LTA, Linde type A zeolite; mA, milli Ampere; min, minutes; ml, milliliter; mol_C, mols on carbon base; N_2, nitrogen; Ni, nickel; $Ni(NO_3)_2$, nickel nitrate; Ni-Ca-LTA, nickel exchanged Ca-LTA; p, pressure; pH, pH value; Pt, platinum; Al_2O_3, aluminum oxide; S, selectivity; SEM, scanning electron microscopy; Si, silicon; SiC, silicon carbide; T, temperature; TGA, thermogravimetric analysis; TOF, turnover frequency; TOS, time on stream; WHSV, weight hourly space velocity; wt.%, weight %; X, conversion; XANES, X-ray absorption near edge structure; XAS, X-ray absorption spectroscopy; XRD, X-ray diffraction; Y, yield;

REFERENCES

((1) Weissermel, K.; Hans-Jürgen, A., *Industrial Organic Chemistry*. Wiley-VCH: Weinheim, 1997.
(2) Albrecht, S.; Kießling, D.; Wendt, G.; Maschmeyer, D.; Nierlich, F. Oligomerisierung von n-Butenen. *Chem. Ing. Tech.* **2005,** 6, 695-709.
(3) Hassan, S. M.; Panchenkov, G. M.; Kuznetsov, O. I. Studies on the Mechanism and Kinetics of Propylene Oligomerization and Hydrooligomerization on Zeolites. *Bull. Chem. Soc. Jpn.* **1977,** 10, 2597-2601.
(4) Ng, F. T. T.; Creaser, D. C. Ethylene Dimerization over Modified Nickel Exchanged Y-Zeolite. *Applied Catalysis A: General* **1994,** 327-339.
(5) Nkosi, B.; Ng, F. T. T.; Rempel, G. L. The Oligomerization of 1-Butene Using NaY Zeolite Ion-Exchanged with Different Nickel Precursor Salts. *Applied Catalysis A: General* **1997,** 1–2, 153-166.
(6) Nkosi, B.; Ng, F. T. T.; Rempel, G. L. The Oligomerization of Butenes with Partially Alkali Exchanged NiNaY Zeolite Catalysts. *Applied Catalysis A: General* **1997,** 1–2, 225-241.
(7) Schultz, R. G.; Engelbrecht, R. M.; Moore, R. N.; Wolford, L. T. Olefin Dimerization over Cobalt-Oxide-on-Carbon Catalysts: II. Butene and Hexene Dimerization. *J. Catal.* **1966,** 3, 419-424.
(8) Skupinska, J. Oligomerization of α-Olefins to Higher Oligomers. *Chem. Rev.* **1991,** 4, 613-648.
(9) Fischer, K.; Jonas, K.; Misbach, P.; Stabba, R.; Wilke, G. Zum „Nickel-Effekt". *Angew. Chem.* **1973,** 23, 1001-1012.
(10) Ziegler, K.; Holzkamp, E.; Breil, H.; Martin, H. Das Mülheimer Normaldruck-Polyäthylen-Verfahren. *Angew. Chem.* **1955,** 19-20, 541-547.
(11) Brückner, A.; Bentrup, U.; Zanthoff, H.; Maschmeyer, D. The Role of Different Ni Sites in Supported Nickel Catalysts for Butene Dimerization under Industry-Like Conditions. *J. Catal.* **2009,** 1, 120-128.
(12) Kumar, N.; Mäki-Arvela, P.; Yläsalmi, T.; Villegas, J.; Heikkilä, T.; Leino, A. R.; Kordás, K.; Salmi, T.; Yu Murzin, D. Dimerization of 1-Butene in Liquid Phase Reaction: Influence of Structure, Pore Size and Acidity of Beta Zeolite and MCM-41 Mesoporous Material. *Microporous Mesoporous Mater.* **2012,** 1, 127-134.
(13) Mlinar, A. N.; Baur, G. B.; Bong, G. G.; Getsoian, A. B.; Bell, A. T. Propene oligomerization over Ni-exchanged Na-X zeolites. *Journal of Catalysis* **2012,** 156-164.
(14) Wendt, G.; Kießling, D. Dimerisierung von n-Butenen an Nickelalumosilicat-Katalysatoren. *Chem. Tech. (Leipzig)* **1995,** 3, 136-143.
(15) Deimund, M. A.; Labinger, J.; Davis, M. E. Nickel-Exchanged Zincosilicate Catalysts for the Oligomerization of Propylene. *ACS Catalysis* **2014,** 11, 4189-4195.
(16) Canivet, J.; Aguado, S.; Schuurman, Y.; Farrusseng, D. MOF-Supported Selective Ethylene Dimerization Single-Site Catalysts through One-Pot Postsynthetic Modification. *JACS* **2013,** 11, 4195-4198.
(17) Madrahimov, S. T.; Gallagher, J. R.; Zhang, G.; Meinhart, Z.; Garibay, S. J.; Delferro, M.; Miller, J. T.; Farha, O. K.; Hupp, J. T.; Nguyen, S. T. Gas-Phase Dimerization of Ethylene under Mild Conditions Catalyzed by MOF Materials Containing (bpy)NiII Complexes. *ACS Catalysis* **2015,** 11, 6713-6718.
(18) Metzger, E. D.; Brozek, C. K.; Comito, R. J.; Dincă, M. Selective Dimerization of Ethylene to 1-Butene with a Porous Catalyst. *ACS Central Science* **2016,** 3, 148-153.
(19) Mlinar, A. N.; Keitz, B. K.; Gygi, D.; Bloch, E. D.; Long, J. R.; Bell, A. T. Selective Propene Oligomerization with Nickel(II)-Based Metal–Organic Frameworks. *ACS Catalysis* **2014,** 3, 717-721.
(20) Brogaard, R. Y.; Olsbye, U. Ethene Oligomerization in Ni-Containing Zeolites: Theoretical Discrimination of Reaction Mechanisms. *ACS Catalysis* **2016,** 2, 1205-1214.
(21) Agirrezabal-Telleria, I.; Iglesia, E. Stabilization of Active, Selective, and Regenerable Ni-Based Dimerization Catalysts by Condensation of Ethene within Ordered Mesopores. *J. Catal.* **2017,** 505-514.
(22) Andrei, R. D.; Popa, M. I.; Fajula, F.; Hulea, V. Heterogeneous Oligomerization of Ethylene over Highly Active and Stable Ni-AlSBA-15 Mesoporous Catalysts. *J. Catal.* **2015,** 76-84.
(23) Beucher, R.; Andrei, R. D.; Cammarano, C.; Galarneau, A.; Fajula, F.; Hulea, V. Selective Production of Propylene and 1-Butene from Ethylene by Catalytic Cascade Reactions. *ACS Catalysis* **2018,** 4, 3636-3640.
(24) Finiels, A.; Fajula, F.; Hulea, V. Nickel-Based Solid Catalysts for Ethylene Oligomerization - A Review. *Catalysis Science & Technology* **2014,** 8, 2412-2426.
(25) Moussa, S.; Arribas, M. A.; Concepción, P.; Martínez, A. Heterogeneous Oligomerization of Ethylene to Liquids on Bifunctional Ni-Based Catalysts: The Influence of Support Properties on Nickel Speciation and Catalytic Performance. *Catal. Today* **2016,** 78-88.
(26) Moussa, S.; Concepción, P.; Arribas, M. A.; Martínez, A. Nature of Active Nickel Sites and Initiation Mechanism for Ethylene Oligomerization on Heterogeneous Ni-beta Catalysts. *ACS Catalysis* **2018,** 3903-3912.
(27) Heveling, J.; Nicolaides, C. P.; Scurrell, M. S. Activity and Selectivity of Nickel-Exchanged Silica-Alumina Catalysts for the Oligomerization of Propene and 1-Butene into Distillate-Range Products. *Applied Catalysis A: General* **2003,** 1, 239-248.
(28) Beltrame, P.; Forni, L.; Talamini, A.; Zuretti, G. Dimerization of 1-Butene over Nickel Zeolitic Catalysts: A Search for Linear Dimers. *Applied Catalysis A: General* **1994,** 39-48.
(29) Cai, T. Studies of a New Alkene Oligomerization Catalyst Derived from Nickel Sulfate. *Catal. Today* **1999,** 1, 153-160.
(30) Sarazen, M. L.; Doskocil, E.; Iglesia, E. Catalysis on Solid Acids: Mechanism and Catalyst Descriptors in Oligomerization Reactions of Light Alkenes. *J. Catal.* **2016,** 553-569.
(31) Sarazen, M. L.; Doskocil, E.; Iglesia, E. Effects of Void Environment and Acid Strength on Alkene Oligomerization Selectivity. *ACS Catalysis* **2016,** 10, 7059-7070.
(32) Sarazen, M. L.; Iglesia, E. Stability of Bound Species During Alkene Reactions on Solid Acids. *Proceedings of the National Academy of Sciences* **2017,** 20, E3900-E3908.
(33) Sarazen, M. L.; Iglesia, E. Experimental and Theoretical Assessment of the Mechanism of Hydrogen Transfer in Alkane-Alkene Coupling on Solid Acids. *J. Catal.* **2017,** 287-298.
(34) Takeuchi, D.; Osakada, K. In *Organometallic Reactions and Polymerization*, Osakada, K., Ed. Springer Berlin Heidelberg: Berlin, Heidelberg, 2014; pp 169-215.
(35) Gal, I. J.; Jankovic, O.; Malcic, S.; Radovanov, P.; Todorovic, M. Ion-Exchange Equilibria of Synthetic 4A Zeolite with Ni2+, Co2+, Cd2+ and Zn2+ Ions. *Transactions of the Faraday Society* **1971,** 0, 999-1008.
(36) Amari, D.; Ginoux, J.-L.; Bonnetain, L. Textural Damage of Cation-Exchanged LTA Zeolites Studied by Gas Adsorption. *Zeolites* **1994,** 1, 58-64.

(37) Rabeah, J.; Radnik, J.; Briois, V.; Maschmeyer, D.; Stochniol, G.; Peitz, S.; Reeker, H.; La Fontaine, C.; Brückner, A. Tracing Active Sites in Supported Ni Catalysts during Butene Oligomerization by Operando Spectroscopy under Pressure. *ACS Catalysis* **2016,** 12, 8224-8228.
(38) Mlinar, A. N.; Shylesh, S.; Ho, O. C.; Bell, A. T. Propene Oligomerization Using Alkali Metal- and Nickel-Exchanged Mesoporous Aluminosilicate Catalysts. *ACS Catalysis* **2013,** 1, 337-343.
(39) Cossee, P. Ziegler-Natta Catalysis I. Mechanism of Polymerization of α-Olefins with Ziegler-Natta Catalysts. *J. Catal.* **1964,** 1, 80-88.
(40) Henry, R.; Komurcu, M.; Ganjkhanlou, Y.; Brogaard, R. Y.; Lu, L.; Jens, K.-J.; Berlier, G.; Olsbye, U. Ethene Oligomerization on Nickel Microporous and Mesoporous-Supported Catalysts: Investigation of the Active Sites. *Catal. Today* **2018,** 154-163.
(41) Mlinar, A. N.; Ho, O. C.; Bong, G. G.; Bell, A. T. The Effect of Noncatalytic Cations on the Activity and Selectivity of Nickel-Exchanged X Zeolites for Propene Oligomerization. *ChemCatChem* **2013,** 10, 3139-3147.
(42) Small, B. L.; Schmidt, R. Comparative Dimerization of 1-Butene with a Variety of Metal Catalysts, and the Investigation of a New Catalyst for C□H Bond Activation. *Chemistry – A European Journal* **2004,** 4, 1014-1020.
(43) Nadolny, F.; Hannebauer, B.; Alscher, F.; Peitz, S.; Reschetilowski, W.; Franke, R. Experimental and Theoretical Investigation of Heterogeneous Catalyzed Oligomerization of a Mixed C4 Stream over Modified Amorphous Aluminosilicates. *J. Catal*. **2018,** 81-94.
(44) Nikiforidis, I.; Görling, A.; Hieringer, W. On the Regioselectivity of the Insertion Step in Nickel Complex Catalyzed Dimerization of Butene: A Density-Functional Study. *J. Mol. Catal. A: Chem.* **2011,** 1–2, 63-70.
(45) F., H. Dimerisation and Double-Bond Isomerisation of Olefins with a Homogeneous Nickel II-Complex as Catalyst. *Journal of Applied Chemistry and Biotechnology* **1971,** 3, 90-91.
(46) Olav-Torgeir, O.; Hagbarth, W.; Ulf, B. Niederdruck-Oligomerisation von Mono-Olefinen mit löslichen Nickel/Aluminium-Bimetallkatalysatoren Teil III. Reaktionskinetische Untersuchungen über die Dimerisation und Trimerisation des Áthylens. *Helv. Chim. Acta* **1969,** 1, 215-223.
(47) Zhang, X.; Zhong, J.; Wang, J.; Zhang, L.; Gao, J.; Liu, A. Catalytic Performance and Characterization of Ni-Doped HZSM-5 Catalysts for Selective Trimerization of n-Butene. *Fuel Process. Technol.* **2009,** 7, 863-870.
(48) Eberly Jr, P. E. High-Temperature Infrared Spectroscopy of Olefins Adsorbed on Faujasites. *The Journal of Physical Chemistry* **1967,** 6, 1717-1722.
(49) Socrates, G., *Infrared and Raman characteristic group frequencies: tables and charts*. John Wiley & Sons: 2001.
(50) Coblentz Society, I. In *NIST Chemistry WEbBook, NIST Standard Reference Database Number 69*, Linstrom, P. J., Mallard, W. G., Eds. National Institute of Standards and Technology: Gaithersburg MD, 20899, 2017.
(51) Armaroli, T.; Finocchio, E.; Busca, G.; Rossini, S. A FT-IR Study of the Adsorption of C5 Olefinic Compounds on NaX Zeolite. *Vib. Spectrosc* **1999,** 1, 85-94.
(52) Kondo, J. N.; Liqun, S.; Wakabayashi, F.; Domen, K. IR Study of Adsorption and Reaction of 1-Butene on H-ZSM-5. *Catal. Lett.* **1997,** 2, 129-133.
(53) Larkin, P. J., *Infrared and Raman Spectroscopy - Principles and Spectral Interpretation*. Elsevier: 2011.
(54) Chang, C. C.; Conner, W.; Kokes, R. Butene Isomerization over Zinc Oxide and Chromia. *The Journal of Physical Chemistry* **1973,** 16, 1957-1964.
(55) Olah, G. A.; Baker, E. B.; Evans, J. C.; Tolgyesi, W. S.; McIntyre, J. S.; Bastien, I. J. Stable Carbonium Ions. V.1a Alkylcarbonium Hexafluoroantimonates. *JACS* **1964,** 7, 1360-1373.
(56) Olah, G. A.; DeMember, J. R.; Commeyras, A.; Bribes, J. L. Stable Carbonium Ions. LXXXV. Laser Raman and Infrared Spectroscopic Study of Alkylcarbonium Ions. *JACS* **1971,** 2, 459-463.
(57) Stepanov, A. G.; Luzgin, M. V.; Romannikov, V. N.; Sidelnikov, V. N.; Paukshtis, E. A. The Nature, Structure, and Composition of Adsorbed Hydrocarbon Products of Ambient Temperature Oligomerization of Ethylene on Acidic Zeolite H-ZSM-5. *J. Catal.* **1998,** 2, 466-477.
(58) Forestière, A.; Olivier-Bourbigou, H.; Saussine, L. Oligomerization of Monoolefins by Homogeneous Catalysts. *Oil & Gas Science and Technology - Rev. IFP* **2009,** 6, 649-667.
(59) Pillai, S. M.; Ravindranathan, M.; Sivaram, S. Dimerization of Ethylene and Propylene Catalyzed by Transition-Metal Complexes. *Chem. Rev.* **1986,** 2, 353-399.
(60) Ravel, B.; Newville, M. ATHENA, ARTEMIS, HEPHAESTUS: Data Analysis for X-Ray Absorption Spectroscopy Using IFEFFIT. *Journal of Synchrotron Radiation* **2005,** 4, 537-541.

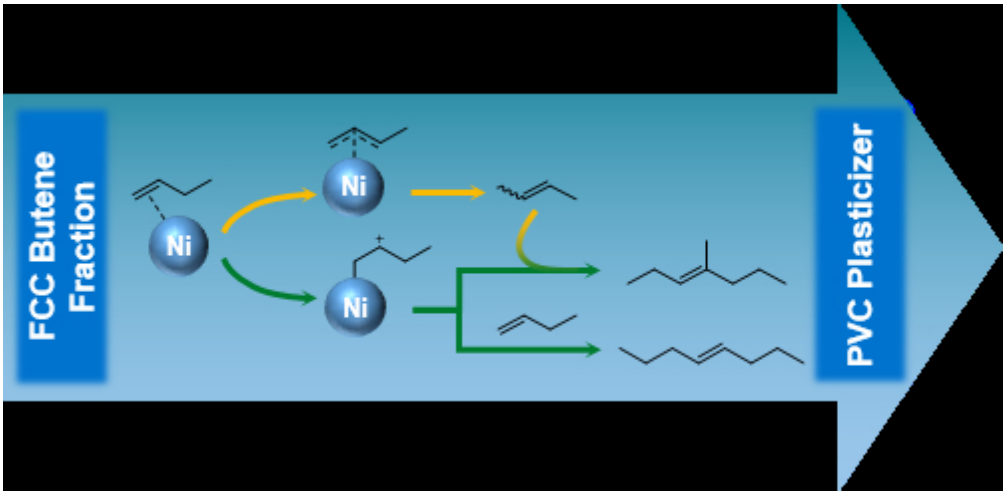

Dimerization of linear butenes on zeolite supported Ni2+

84x41mm (150 x 150 DPI)